ICES Journal of Marine Science

ICES International Council for the Exploration of the Sea
CIEM Conseil International pour l'Exploration de la Mer

ICES Journal of Marine Science (2018), doi:10.1093/icesjms/fsy164

Adapting the dynamic energy budget (DEB) approach to include non-continuous growth (moulting) and provide better predictions of biological performance in crustaceans

S. Elizabeth Talbot[1,2*], Stephen Widdicombe[1], Chris Hauton[2], and Jorn Bruggeman[1]

[1]*Plymouth Marine Laboratory, Prospect Place, West Hoe, Plymouth PL1 3DH, UK*
[2]*Ocean and Earth Science, National Oceanography Centre Southampton, University of Southampton Waterfront Campus, European Way, Southampton SO14 3ZE, UK*

**Corresponding author: tel: +44 (0)1752 633486; e-mail: sat@pml.ac.uk*

Talbot, S. E., Widdicombe, S., Hauton, C., and Bruggeman, J. Adapting the dynamic energy budget (DEB) approach to include non-continuous growth (moulting) and provide better predictions of biological performance in crustaceans. – ICES Journal of Marine Science, doi:10.1093/icesjms/fsy164.

Received 23 March 2018; revised 5 September 2018; accepted 11 October 2018.

Dynamic energy budget (DEB) theory offers a comprehensive framework for understanding the overall physiological performance (growth, development, respiration, reproduction, etc.) of an organism over the course of its life cycle. We present here a simplified DEB model for the swimming crab *Liocarcinus depurator*. To the best of our knowledge, this is the first to be presented for this species. Most applications of the standard DEB model assume continuous growth in all size metrics (length, wet mass, carbon content) of the modelled species. However, in crustaceans growth, measured as an increase of carapace length/width, occurs periodically via moult. To account for this, we have extended the model to track the continuous increase in carbon mass as well as the episodic increase in physical size. Model predictions were consistent with the patterns in the observed data, predicting both the moult increment and the intermoult period of an individual. In addition to presenting the model itself, we also make recommendations for further development, and evaluate the potential applications of such a model, both at the individual level (e.g. aquaculture) and as a potential tool for population level dynamics (e.g. fisheries stock assessment).

Keywords: Keywords: crustacean growth, dynamic energy budget, metabolic theory, moulting.

Introduction

The implications of anthropogenic climate change for marine ecosystems are profound (Harley *et al.*, 2006). A key challenge for marine scientists is to measure and predict the magnitude and rapidity of the effects of climate change on these ecosystems and the economic and social systems that depend on them. While there are studies documenting climate-related mortality events (Hoegh-Guldberg, 1999; Harley and Paine, 2009), shifts in species range boundaries (Zacherl *et al.*, 2003; Hiddink and Ter Hofstede, 2008; Poloczanska *et al.*, 2013) and phenological shifts in the timing of reproductive events (Poloczanska *et al.*, 2013), a comprehensive mechanistic understanding of these events has so far been lacking (Pörtner and Knust, 2007; Bozinovic and Pörtner, 2015). Given the numerous studies showing that physiological tolerance varies geographically (Helmuth *et al.*, 2006; Place *et al.*, 2008; Pearson *et al.*, 2009), it is clear that a more thorough understanding of the mechanisms underlying the interactions between changes in the physical environment and organismal and ecological responses are critical if we are to predict future patterns of biodiversity, distribution, and abundance. This predictive capability is particularly important for species of commercial interest, those that provide important ecosystem services such as coastal protection or waste remediation, and those taxa that play a key ecological role within an ecosystem, for instance as habitat providers.

Crustaceans, particularly decapods, have important ecological roles (Boudreau and Worm, 2012). Studies have shown that decapod predation can influence the structuring of benthic communities (Quijón and Snelgrove, 2005), and that crustacean predators can be keystone species, regulating the density of herbivorous prey species and indirectly maintaining complex habitats such as salt marshes (Silliman and Bertness, 2002) and kelp beds (Leland, 2002; Steneck *et al.*, 2004).

Some crustacean species, such as clawed and spiny lobster, crabs, and penaeid shrimp, also have significant commercial value (Smith and Addison, 2003). These decapods underpin lucrative fisheries across the globe and deliver some of the highest prices per weight of any seafood (Cawthorn and Hoffman, 2017). Global production of decapod crustaceans has doubled since 2000, reaching over 12.5 million tonnes in 2013 and accounting for approximately 8% of total global fisheries production (Cawthorn and Hoffman, 2017). While landings from decapod capture fisheries have remained relatively stable over the last decade, the rapid increase in global supply largely reflects the growth in aquaculture production, predominantly in Asia. In 2014, aquaculture production of crustaceans reached 6.9 million tonnes, worth an estimated US$36.2 million (FAO, 2016).

The moult cycle represents a major and repeated physiological change in the life history of all crustaceans (Buchholz *et al.*, 2006; Seear *et al.*, 2010). Given that moulting is a complex and energy-demanding process, most aspects of crustacean life history are synchronized with the moult cycle (Raviv *et al.*, 2008). Both reproduction and metabolism are dependent on the moult stage in crustaceans, and all three phenomena—moult, reproduction, and metabolism—are influenced by environmental factors such as temperature (Buchholz *et al.*, 2006). Moult and reproduction can be coordinated in a variety of ways, with different reproductive events (e.g. mating and oviposition) coupled to different moult stages (Cuzin-Roudy and Buchholz, 1999; Buchholz *et al.*, 2006). Since mating can indicate the onset, acceleration or completion of vitellogenesis, and since oviposition marks the beginning of egg incubation, the sequence of mating and oviposition combined with the occurrence of moulting comprise different reproductive strategies (Raviv *et al.*, 2008). Some of these strategies can be related to a particular taxon, while others may be found in a variety of taxa. Furthermore, a single species may exhibit more than one reproductive strategy. For example, in the snow crab *Chionoecetes opilio* (Fabricius, 1788) the first reproductive cycle comprises pre-moult ovary maturation, followed by the pubertal (and terminal) moult. Copulation occurs with the female in a soft shelled condition and the cycle ends with oviposition. In all subsequent reproductive cycles mating and oviposition occur with the female in a hard shelled condition (Elner and Beninger, 1995; Sainte-Marie *et al.*, 2008). The reproductive cycle is regulated by a combination of internal cues such as energy allocation, and external environmental cues such as season (Raviv *et al.*, 2008).

As well as facilitating growth and reproduction, moult may also be undertaken as a response to stressors or parasite infection. For example, Antarctic krill *Euphausia superba* (Dana, 1850) have the capacity to shrink at moult under conditions of low food availability (Ettershank, 1983; Nicol *et al.*, 1992; Nicol, 2000). It is possible that this mechanism would allow the species to survive a long period of food limitation such as that encountered during the Antarctic winter (Quetin and Ross, 1991). Similarly, the Northern Krill *Meganyctiphanes norvegica* (M. Sars, 1857) moults outside of the reproductive season, and shows negligible somatic growth. It has been proposed that these moults may remove ecto-parasites that can severely reduce swimming efficiency (Buchholz *et al.*, 2006).

Modelling growth forms the basis for almost all quantitative fisheries stock assessment (Chang *et al.*, 2012). Accurate estimates of growth are essential in the determination of lifespan, age at recruitment, age at maturity, and cohort identification (Hoggarth, 2006; Chang *et al.*, 2012). Similarly it is critical for aquaculture production of crustaceans. Not only does it allow producers to assess when a crop will be ready for harvesting, but it also provides a way of quantifying and evaluating the effects of different production systems (Wyban *et al.*, 1995; Kim *et al.*, 2014), dietary regimes (Ackefors *et al.*, 1992), or immunostimulants (Bai *et al.*, 2010; Sang *et al.*, 2011) on growth.

Moulting in crustaceans causes two problems in quantifying growth: all hard parts that might be used for aging (and so for an estimation of size at age) are lost at each moult, and growth is discontinuous, occurring in a stepwise fashion (Chang *et al.*, 2012). While the first of these problems may be overcome by using methods such as mark recapture data (for larger or slower growing species) or length frequency analysis (Kilada and Driscoll, 2017) to estimate relative size at age, the second problem of discontinuous growth has received less attention, and limited attempts have been made to model the stepwise growth of crustaceans (Chang *et al.*, 2012).

In order to capture moult dynamics in crustaceans, information on two components is needed—the moult increment (MI) (i.e. the magnitude of the increase in size at moult), and the intermoult period (IP) (i.e. the length of time between two successive moults) (Chang *et al.*, 2012). The MI is generally the simpler of the two processes to model, with much of the modelling effort focused on finding the best means of fitting pre-moult and post-moult size data. These range from the fitting of separate lines to pre- and post-moult data with an intersection corresponding roughly to the size at maturity (Somerton, 1980), to log-linear (Mauchline, 1977) or non-linear models (Easton and Misra, 1988). Modelling the IP is more of a challenge, as the only way to measure it directly is by observing animals in captivity. In those studies that have recorded data on observed IP, various general functions relating IP to pre-moult size have been proposed. For example, simple and higher order linear models (Mauchline, 1977; Castro, 1992), non-linear models (Ehrhardt, 2008), and a geometric series of time intervals increasing from an initial "seed" interval by a constant proportion at each successive interval (Caddy, 2003) have all been used. In those studies that have no direct measurement of IP, an estimate of moulting probability or moulting frequency is required, and many empirical equations exist to relate moulting probability to pre-moult size (Chang *et al.*, 2012). Once information on MI and IP has been obtained, there are various ways of quantifying the average growth versus time. The moult-process model projects the relationship between pre-moult size and MI, and pre-moult size and IP repeatedly, allowing for the prediction of growth beyond the size range of the original observations (Mauchline, 1977). This approach is deterministic however, and does not account for intrinsic variations in growth among individuals. A stochastic moult-process model has therefore been developed based on the Monte-Carlo technique to construct growth curves and their associated uncertainty (Chen and Kennelly, 1999). While both these models produce growth curves, neither of them consider the effect of environmental factors on growth.

While all of these methods have been used successfully to model growth in a number of crustacean taxa, the fact that many

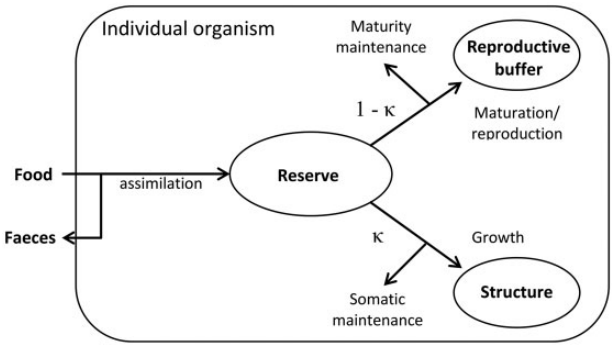

Figure 1. Schematic diagram of the standard DEB model. State variables are in ovals. κ (kappa) is the energy allocated to somatic maintenance and growth and represents a fixed fraction of energy mobilized from the reserve. $1-\kappa$ is the remainder of mobilised energy and is allocated to either maturation (juveniles) or reproduction (adults). Mature animals sink energy into the reproductive buffer until it is emptied during reproductive events (i.e. gamete release).

of them have been developed for a particular species means it is unlikely that any individual model will be applicable to all species. Additionally, while some of them explicitly consider the effects of environmental temperature on growth (Wainwright and Armstrong, 1993; Brylawski and Miller, 2006) none consider food availability. In order to simplify the process of modelling crustacean growth, and to facilitate comparisons of growth between species, a single mechanistic model that can quantify both MI and IP, relate both to environmental temperature and food availability, and which should be applicable to all crustacean species is required.

Dynamic energy budget (DEB) models offer a whole organism approach to explain how factors in the physical environment translate into biologically and ecologically relevant responses, via the assumption that food and temperature are the primary drivers of an organism's metabolic machinery. DEB models are based on the assumption that assimilated energy is first stored in reserves, which are then mobilized to fuel other metabolic purposes (van der Meer, 2006). The standard "κ-rule" (kappa rule) DEB model (Figure 1) states that a fixed fraction (κ) of mobilized energy is allocated to maintenance and growth, and the remaining fraction $(1-\kappa)$ is available for development and reproduction (van der Meer, 2006).

In the standard DEB model (Figure 1), individuals are assumed to be isomorphs (no ontogenetic changes in body shape) feeding on one food source (Jager and Zimmer, 2012). They are primarily characterized by three state variables: structure, which is linked to metrics such as body/carapace length, feeding rates, and maintenance costs; reserve, which serves as intermediate storage between feeding and metabolic mobilisation, and either maturation (in juvenile animals) or reproduction buffer (in sexually mature animals) (Martin *et al.*, 2013).

Application of the DEB model to crustaceans has some specific challenges. The standard DEB model assumes continuous growth of structure (Figure 1). In most animal phyla, an increase in structure results in a concurrent increase in physical size (e.g. body length). However, this is not the case with crustaceans in which growth of structure is indeed continuous, but increase in physical size occurs periodically via the moult. In most of the published DEB models which apply to crustaceans (Nisbet *et al.*, 2004; Campos *et al.*, 2009; Jager *et al.*, 2015; Jager and Ravagnan, 2015, 2016), these discontinuities in physical size measures are ignored. The single exception known to us is the work of Ananthasubramaniam *et al.* (2015), which includes explicit representation of discrete moults in *Daphnia magna* using a moult development index. The assumption that model predictions are representative of overall growth over multiple moults rather than individual daily growth is not unreasonable when dealing with relatively small fast growing crustacean species that moult frequently (Campos *et al.*, 2009; Jager and Ravagnan, 2015), but when dealing with larger bodied, longer lived species such as commercially important decapods, it is less representative. It is possible, in the case of these decapods, that any modelled process which depends upon the physical size of the animal (e.g. feeding) is not accurately represented.

This study aims to investigate the feeding, growth, and respiration of a common marine crustacean, *Liocarcinus depurator* (Linnaeus, 1758), and to parameterize a simple DEB model in order to explore the energy budget of this species. Additionally, we test the skill of this DEB model in capturing both the MI and the IP. As far as we are aware, this model is the first DEB model to be presented for *Liocarcinus depurator*.

Material and methods

Animal collection

Individuals of *Liocarcinus depurator* were collected on 9 June 2016 from the Western Channel Observatory (Smyth *et al.*, 2015) sampling station L4 (50°15.00′N, 4°13.02′W) using a 2 m beam trawl. Four separate trawls, each of 15 min duration, were conducted to ensure collection of a sufficient number of individuals ($N=60$). Once removed from the cod end of the trawl, all intact individuals were transferred into buckets of freshly collected seawater (vol = 5 l, five individuals per bucket) and transported back to Plymouth Marine Laboratory (PML, Plymouth, UK) within 2 h of collection.

On arrival back at PML, animals were transferred to individual plastic containers (vol = 1 l) filled with filtered (10 µm) seawater and placed in the mesocosm tanks, two large (vol = 600 l) tanks of seawater maintained at 10°C ± 0.5°C. Each individual plastic container had a layer of aquarium gravel (Dennerle Plantahunter, 8–12 mm, J & K Aquatics) for the animal to sit on, and was aerated individually, with air being finely bubbled through aquarium airstones. Once transferred to these containers, individuals were left for 48 h prior to the start of the experiment.

Experimental design

In the first week of the experiment, each individual's carapace width (CW) was measured with digital Vernier calipers (±0.05 mm) and then weighed on a balance scale (Sartorius R220-D, 0.01 mg, European Instruments). These measurements were repeated weekly for the duration of the experiment (10 weeks). Once a week, the containers were washed, the gravel rinsed with clean seawater, and the water was changed. *Liocarcinus* were fed three times per week (Monday, Wednesday, and Friday) on raw squid tubes (*Illex argentinus*). Wet weight of squid (typically between 1 and 1.5 g) was measured before being presented to the animals, which were then left undisturbed for 6 h to feed. After the 6 hr period, any un-ingested squid was removed and reweighed.

Oxygen consumption data were collected for randomly selected individuals during the last 3 weeks of the experiment. *Liocarcinus* were removed from their individual containers and placed on a platform in a 920 ml static respiration chamber containing aerated seawater of the same temperature as that in the experimental aquaria. The chamber was placed on a stirrer plate and a 10 mm stir bar mixed the water at 500 rpm, separated from the animal by the platform. The rpm was kept at the lowest possible setting to ensure that water in the chamber would be mixed while minimizing disturbance to the animal. The chamber was then covered with a black cloth and the crab left to settle for approximately 30 min (the time it took for the animal to stop moving around the chamber or displaying obvious signs of agitation such as climbing the sides). After this initial 30 min period, the chamber was sealed, ensuring there were no trapped air bubbles, and an initial measurement of the percentage air saturation in the chamber was taken using an OxyMini-AOT (World Precision Instruments). Further measurements were taken every 15 min for up to 3 h, with the chamber covered with a black cloth between measurements to ensure the crabs experienced minimal disturbance. At no point during the measurements was air saturation in the chamber allowed to drop below 70%. Percent air saturation was converted to μmol O_2 l^{-1} using the formula:

$$\left[\frac{P_{\text{atm}} - P_{\text{w}}(T)}{P_{\text{N}}} \cdot \frac{\%\ \text{air saturation}}{100}\right.$$

$$\left. \cdot 0.2095 \cdot \alpha(T) \cdot 920 \cdot \frac{M(\text{O}_2)}{V_{\text{m}}}\right] \cdot 31.25$$

where P_{atm} is atmospheric pressure (mbar)

P_{N} is standard pressure (1013 mbar)

$P_{\text{w}}(T)$ is vapour pressure of water (Pa) at measurement temperature (K)

is the Bunsen absorption coefficient at measurement temperature (K)

$M(O_2)$ is the molecular mass of O_2 (32 g/mol)

V_{m} is the molar volume (22.414 l/mol)

0.2095 is the volume content of O_2 in air

31.25 is the conversion factor from mg l^{-1} to μmol l^{-1}

and 920 is the volume of the respirometry chamber (ml)

Subsequently, the rate of whole animal O_2 consumption (μmol O_2 consumed min^{-1}) was determined by plotting μmol O_2 over time for each crab, and calculating the slope of the regression line. To allow for a more accurate comparison of O_2 consumption rates between individuals of different sizes, O_2 consumption was then corrected to μmol O_2 consumed g wet mass $(M_W)^{-1}$ min^{-1}.

Wet mass/carbon mass conversions

Prior to collection of experimental animals, ~80 individuals were collected from the same location, following the same method outlined above. These animals were euthanized on arrival at PML by immersing them in briny water chilled to −11°C and then weighed and measured in the same way as the experimental animals. Once wet mass had been established, individuals were placed in a drying oven at 60°C and dried to a constant weight (typically 48 h), left to cool to room temperature in a desiccator (typically 2–3 h) and weighed again on removal to quantify dry mass. Animals were then placed in a muffle furnace at 550°C for 4 h to be incinerated (West *et al.*, 2004), and the remaining ash weighed. Carbon mass was calculated by subtracting the ash weight from the dry weight. The ratio of carbon mass to wet mass was then calculated.

Liocarcinus depurator DEB model structure

A simplified version of the standard DEB model was implemented in the R programming environment and used to evaluate growth, ingestion, and oxygen consumption in *Liocarcinus depurator* (see Figure 2 for an outline of the model procedure). In terms of the simplification of the standard DEB model, all carbon allocated to maturation and reproduction, as defined by the "kappa rule", was respired completely in this model. This decision was made because observations on maturity of the individuals and on the biomass of their reproductive tissues was lacking; furthermore, it allowed the same model to be used for juvenile and mature individuals, without having to detect the moment of maturation. This makes the model equivalent to that of a standard DEB juvenile animal. As a result, modelled total biomass by necessity excludes reproductive tissues; for modelled oxygen consumption, the oxygen needed to metabolize all carbon allocated to maturation/reproduction was included. For mature animals the model has the potential to slightly underestimate total mass, and overestimate respiration. However, we believe this is a reasonable simplification, given the small size of crabs involved, and the absence of eggs in all animals.

Given the discontinuous nature of crustacean growth, and the potential difference in tissue composition that can be measured in two animals of the same CW, carbon mass (M_C) was identified as a more appropriate size metric to use in order to quantify the model's continuously varying state variables, structure (M_V), and reserve (M_E) (NB: any use of the term "structure" in this article refers to the state variable M_V). However, as M_C cannot be measured directly without sacrificing experimental animals, the model was extended with a variable for wet mass (M_W), an easily established measure of physical size. This variable was designed to change only through moulting. The moulting process was triggered when the modelled ratio of carbon mass to wet mass (α) exceeded a threshold calculated from observed carbon to wet mass ratios (Figure 3 and *Carbon mass/wet mass* in Results section). We note that α increased between moults due to assimilation of carbon (and increased structure and reserve), while M_W remains fixed (equation ix). In this way, the model produced a stepwise growth curve in wet mass, even though structure and reserve increased continuously, with α as the primary link between the measured variable M_W, and the state variables M_V and M_E. This increase in M_V and M_E, taken alongside the constant M_W between moults, implies a change in water content of the animal during the IP.

In DEB theory, ingestion scales with surface area, assumed to be proportional to structure$^{2/3}$ in the standard DEB model. This reflects the idea that ingestion is a function of the surface area of organs responsible for ingestion and/or digestion. However, in moulting animals the physical size of organisms remains constant between moults, and is more appropriately measured by wet mass than the carbon mass of structure. Therefore, we assume that the surface areas responsible for ingestion, and thus, the maximum ingestion rate, are proportional to $M_W^{2/3}$ (equation iii). To test the validity of this assumption, we examined the log–log relationship

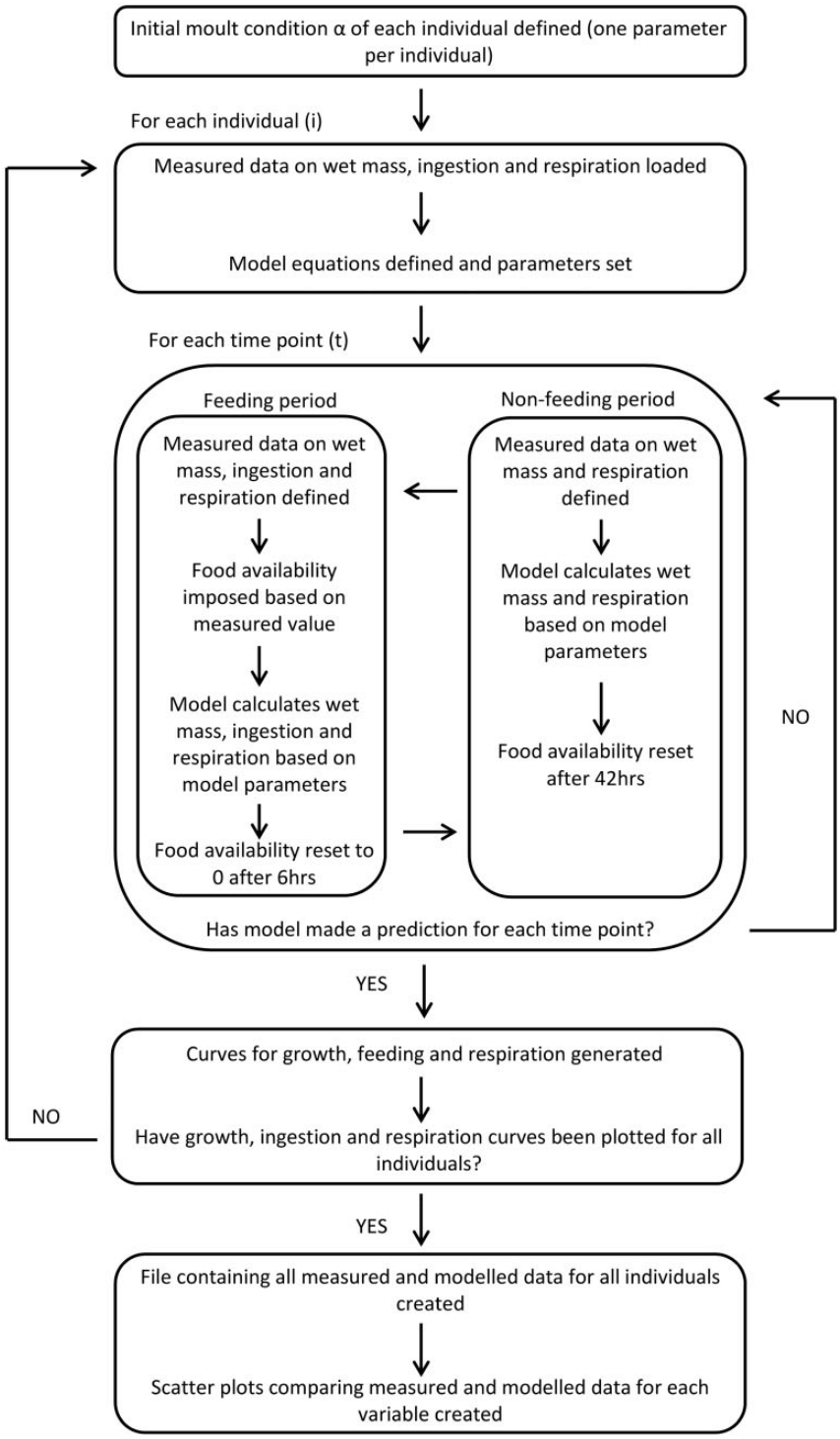

Figure 2. Flow chart outlining the major steps of each model iteration in R statistical software. Initial moult condition is the parameter α. Note that the model was designed to differentiate between feeding and non-feeding periods. All code was developed *de novo*, although the majority of the model equations are from the standard DEB model. Any exceptions are listed in the section "Model equations and parameter values".

between wet mass and measured ingestion rate (Figure 4), and found that ingestion scales to $M_W^{0.65}$. Other size-dependent processes in the DEB standard model, specifically the reserve mobilization rate and the maintenance rate, were left to scale with structure, as these are thought to relate primarily to metabolically active biomass and energy density, rather than physical size.

Additional logic to describe the feeding regime was introduced as part of the model code, in which the simulation was cut into

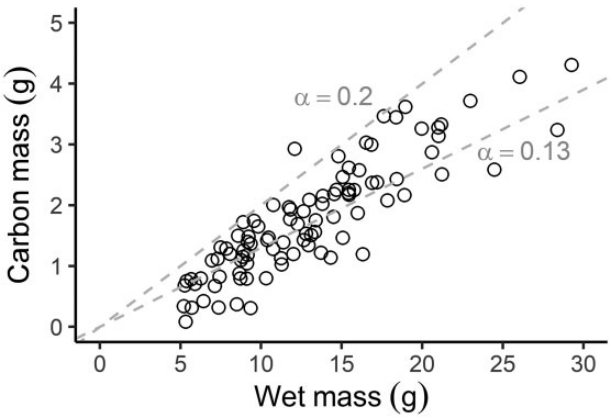

Figure 3. Carbon mass/wet mass ratio (α) for *Liocarcinus depurator*. The two dashed lines represent the best fitting model for the upper and lower envelope (for derivation, see Supplementary Material). The lower dashed line represents the approximate α of a newly moulted crab (0.13); the upper dashed line represents the "moult threshold" of 0.2. Once an animal reaches this threshold it will moult in the model.

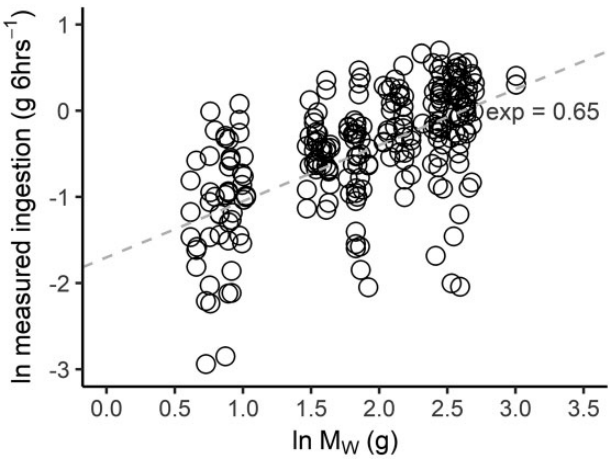

Figure 4. Log–log relationship between wet mass (M_W) and ingestion in *Liocarcinus depurator*. Measured ingestion scales with $M_W^{0.65}$.

many feeding and non-feeding periods that are individually simulated and linked through the initial and final states of the individual being modelled. The model calculated the amount of food ingested over the 6 h feeding period, based on the maximum ingestion rate scaled to $M_W^{2/3}$ (equation iii). It then compared the modelled output to the measured output.

Model equations and parameter values

Most model equation equations are standard DEB model equations (Kooijman, 2010), although we do not entirely adhere to the commonly used notation. For example, our decision to use M_W as our measure of physical size necessitated the calculation of certain parameters (e.g. energy conductance, v) in $g^{1/3}\ d^{-1}$, rather than cm d^{-1}. We also calculate all fluxes in g d^{-1}, rather than in J or C-moles d^{-1}. Some equations needed to be adjusted to accommodate our chosen size measure. In equation (iii), ingestion scales with M_W rather than surface area, and equation (viii) is a cubic function (not part of standard DEB) to calculate the initial state of structure M_V. Equation (ix) is a new equation which calculates the magnitude of wet mass increase during a moult.

State variables are structure M_V and reserve M_E

(i) Reserve density (gC gC^{-1})

$$m_E = \frac{M_E}{M_V}$$

(ii) Functional response for ingestion

$$f = \frac{X}{X + K}$$

where X is food and K is the half saturation coefficient. At *ad libitum* food, $f = 1$

(iii) Ingestion ($gM_W\ d^{-1}$)

$$J_{XA} = \{j_{XAm}\}\ M_W^{\frac{2}{3}}\ f$$

Where $\{j_{XAm}\}$ is the maximum ingestion rate scaled to $M_W^{2/3}$

(iv) Assimilation (gC d^{-1})

$$J_{EA} = y_{EX}\ J_{XA}$$

Where y_{EX} is the assimilation efficiency

(v) Specific growth rate (d^{-1}) of structure M_V (gC)

$$r = \frac{y_{VE}\left[\kappa m_E \frac{v}{L} - k_M\right]}{1 + y_{VE}\kappa m_E}$$

Where y_{VE} is growth efficiency when turning reserve into structure and v ($g^{1/3}\ d^{-1}$) is the reserve turnover rate
L is the structural length ($g^1/_3$), which equals $\sqrt[3]{M_V}$
k_M is the maintenance cost (d^{-1}) and
κ is the energy allocated to somatic maintenance and growth

(vi) Catabolic flux (reserve mobilisation) (gC d^{-1})

$$J_{EC} = M_E\left(\frac{v}{L} - r\right)$$

(vii) Respiration (CO_2 flux in gC d^{-1}) is equal to all carbon mobilized from the reserve, minus the carbon used in growth (i.e. fixed in structural biomass)

$$resp = J_{EC} - (r \cdot M_V)$$

Note that this includes all carbon allocated to maturation and/or reproduction.

(viii) Due to the use of M_W as an indicator of physical size, the calculation used in the standard DEB model to determine

Table 1. Mean parameter values for *Liocarcinus depurator*, along with values for the shore crab *Carcinus maenas* (taken from the Add my Pet database) for comparison.

Parameter	Symbol	Values ± SD	*Carcinus maenas* values	Unit
Maximum ingestion rate scaled to $M_W^{2/3}$	j_{XAm}	1.41 ± 0.24	–	$g^{1/3}\,M_W\,d^{-1}$
Assimilation efficiency	y_{EX}	0.87 ± 0.08	0.8	–
Energy conductance	v	0.03 ± 0.01	0.02*	$g^{1/3}\,C\,d^{-1}$
Fraction of energy allocated to somatic maintenance and growth	κ	0.9 ± 0.02	0.9	–
Somatic maintenance rate	k_M	0.07 ± 0.03	0.09	d^{-1}
Growth efficiency	y_{VE}	0.65 ± 0.04	0.8	–

*Values for energy conductance in *C. maenas* were originally measured in cm d^{-1}. The value reported here has been converted to $g^{1/3}$ C d^{-1} using a conversion factor of 1.7.

the initial state of structure M_v is not applicable and is replaced with the cubic function

$$x^3 + c_1\ x - \ c_2 = 0$$

Where $x = \ M_V{}^{1/3}$ and

$$c_1 = \frac{\{j_{XAm}\}M_W^{\frac{2}{3}}\ f}{v}$$

$$c_2 = \frac{M_W}{(M_W/M_C)}$$

For full derivation and assumptions, see Supplementary Material.

(ix) During a moult, triggered by the ratio of carbon (structure + reserve) to wet mass (α) reaching the predefined maximum α_{pre}, water is taken in until α reaches the predefined minimum α_{post}. Therefore, M_W post moult is calculated as

$$M_{W\,new} = \frac{M_W\ \cdot\ \alpha_{pre}}{\alpha_{post}}$$

Parameter values are listed in Table 1. Initial values for energy conductance (v), fraction of allocation to soma (κ) and volume specific maintenance costs (k_M) were obtained from the DEB species explorer (Bruggeman, 2017). Ingestion rate $\{j_{XAm}\}$ was calculated for each animal from observed data. Initial values for assimilation efficiency (y_{EX}) and growth efficiency (y_{VE}) were estimated from the literature (Klein Breteler, 1975; Paul and Fuji, 1989; Iguchi and Ikeda, 1995, 2004; Lemos *et al.*, 2001; Taylor and Peck, 2004; McGaw and Whiteley, 2012). As there is little data on assimilation and growth efficiency in *L. depurator* specifically, these values were estimated from assimilation and growth efficiency data from a range of predatory decapod crustaceans. The model was run with these parameters and predictions for growth, ingestion and O_2 consumption were compared to measured values for each individual crab. Model performance was assessed using mean absolute error (MAE), a standard model test statistic which gives equal weight to all errors and as such is easy to interpret. All parameters except j_{XAm} (for which there was a calculated value for each crab) were then tuned, by hand, the model iterated again, and performance assessed using MAE for each individual. This process was repeated until a parameter set was found for each individual which minimized the deviation between predictions and observations for the three metrics investigated (growth, ingestion, and O_2 consumption), based on the MAE. The mean values of all parameters were then calculated, and the model run for a final time using these mean parameter values and observations from all experimental animals. Validity of the parameters was assessed by comparing them to a parameter set for the related portunid crab *Carcinus maenas* (Linnaeus, 1758), taken from the Add my Pet database (AmP, n.d.). While a certain level of deviation between parameter estimates for the two species is to be expected, we assume that their relative taxonomic proximity would result in similar values (e.g. for the values for *C. maenas* to be within 1 *SD* of the mean parameter values for *L. depurator*).

In order to facilitate a comparison between this model, in which moult dynamics are explicitly considered, and the standard DEB model, in which physical size is allowed to increase constantly alongside the increase in structure and reserve, the model was run again without the "moult extension" applied. In this version of the model, ingestion was scaled to structure, rather than $M_W^{2/3}$.

Results

Carbon mass/wet mass

Carbon mass/wet mass ratios (α) in animals collected from the field were found to range from ~0.13 to ~0.2 (Figure 3, see Supplementary Material for full derivation of the fitting procedure for the upper and lower envelope). These extremes describe the "moult condition" in *Liocarcinus*, with newly moulted individuals having a α of ~0.13, and individuals approaching a moult having a α of ~0.2. These ratios were imposed in the DEB model, where they control both the timing of the moult and the magnitude of the increase in wet mass.

Scaling of ingestion to wet mass

Measured ingestion was found to scale approximately with $M_W^{2/3}$. The actual exponent was 0.65 (Figure 4).

Growth, ingestion, and oxygen consumption

Figure 5 illustrates the skill of the DEB model in predicting both the timing of the moult and the magnitude of the increase in wet mass for all of those individuals which moulted over the course of the experiment. The structure of the animal (dotted black line) changes smoothly between moults, while wet mass increases in a stepwise manner. The dynamics of the reserve are also apparent (grey line), with reserve increasing after food has been assimilated, and decreasing as it is mobilized for somatic growth and maintenance. In some cases, the model underestimates the increase in wet mass (Figure 5a, f, h, and k). In two cases, it lacks accuracy in predicting the timing of the moult (Figure 5a and f). As noted in the Material and Methods section, the model does have the capacity to slightly underestimate total biomass due to the fact that modelled biomass excludes reproductive tissues.

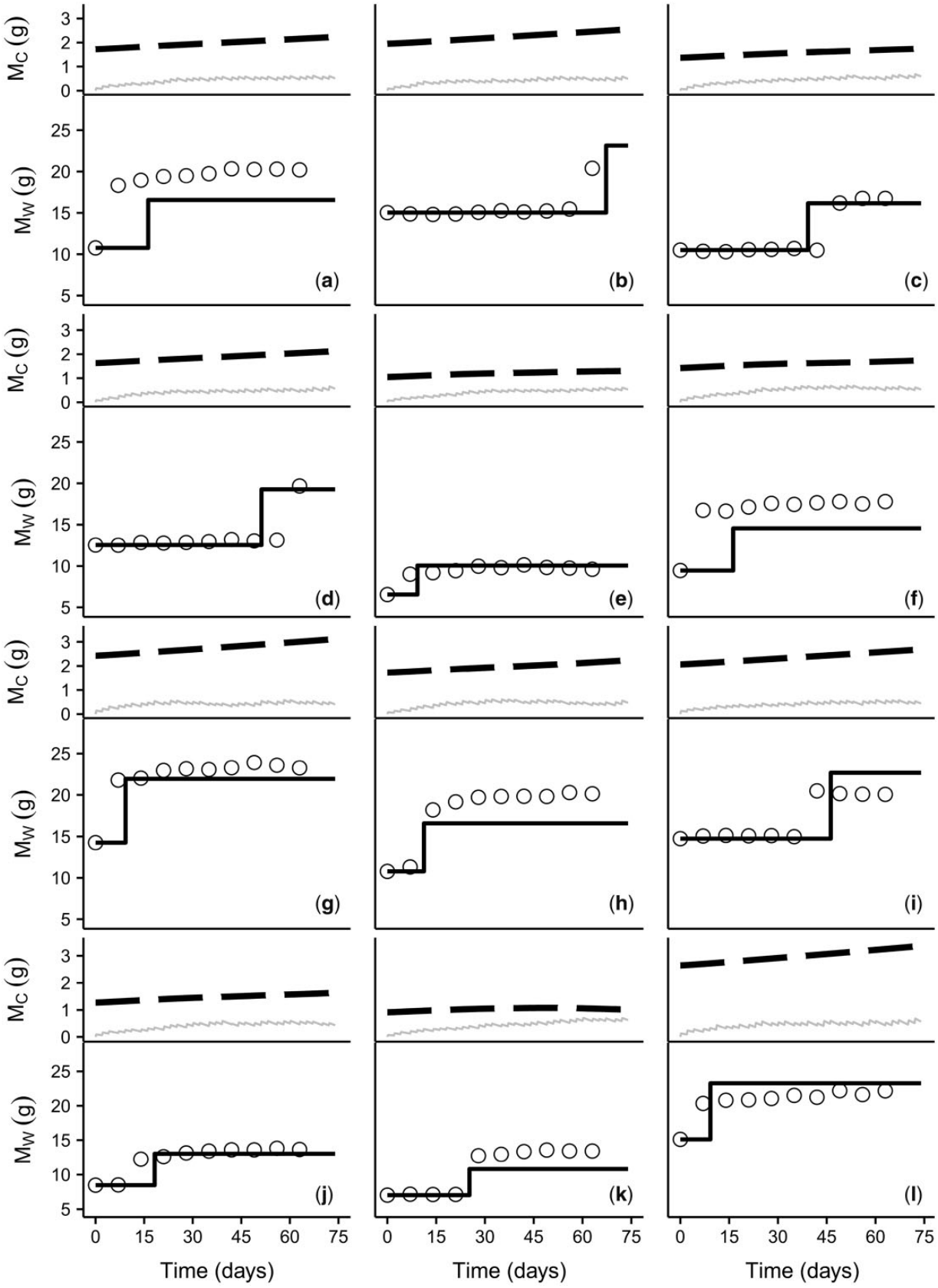

Figure 5. Growth curves for all those animals which moulted over the course of the experiment. Black circles are measured wet mass, solid black line is modelled wet mass. Dashed black line is modelled structure, and solid grey line is modelled reserve (both measured in g carbon). The zig-zag appearance of the grey line is a reflection of the reserve dynamics. Reserve increases as food is assimilated, and decreases as it is mobilized for somatic growth and maintenance. The upward trend of the dashed black line is the overall increase in structure. Note how structure increases smoothly while wet mass increases in a stepwise fashion.

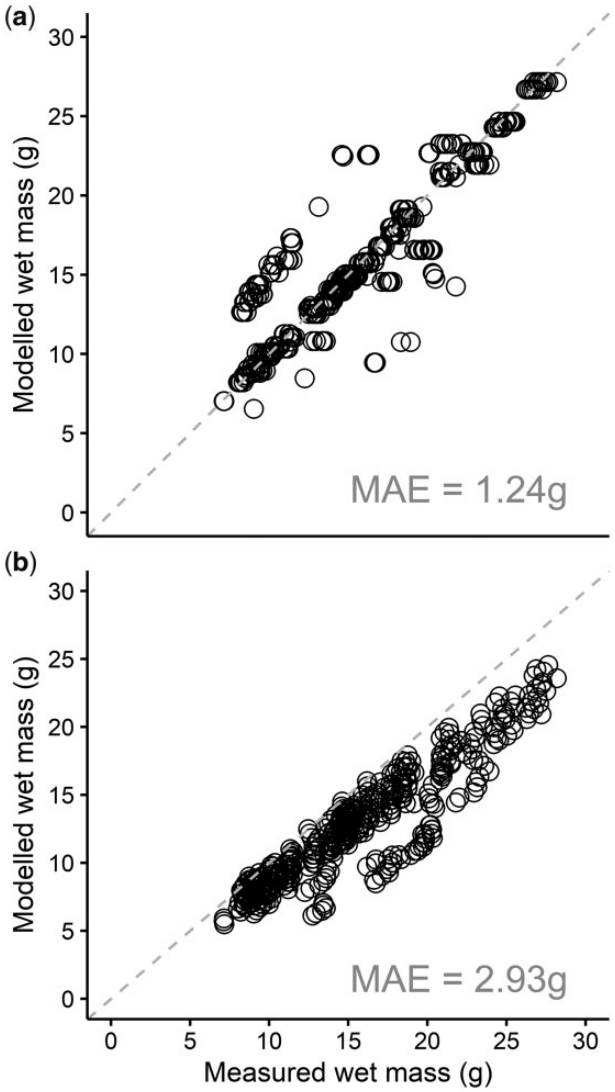

Figure 6. Measured versus modelled wet mass in *Liocarcinus depurator*. (a) Shows performance of the model with the "moult extension" presented here. (b) is the performance of the model when run as a standard DEB model, without the dynamics of the moult considered. Dashed line is a 1:1 reference line. Modelled values were calculated using the parameter values in Table 1. Mean average error (MAE) is shown.

A direct comparison of modelled and measured wet masses for all experimental animals ($N = 52$, data for those animals which died over the course of the experiment were not considered) shows overall model skill is good, with a MAE of 1.24 g (Figure 6a). Those points which sit on the 1:1 reference line represent each time step at which measured and modelled wet masses matched. The points sitting above and below the reference line represent those time steps at which modelled and measured wet masses differed. These mismatches are largely due to the model either underestimating wet biomass (Figure 5a, f, h, and k), or a lack of accuracy in predicting moult timing (Figure 5a and f). The performance of the model when run as a standard, if simplified, DEB model (i.e. without the "moult extension", allowing M_W to increase continuously) is poorer, with a MAE of 2.93 g (Figure 6b).

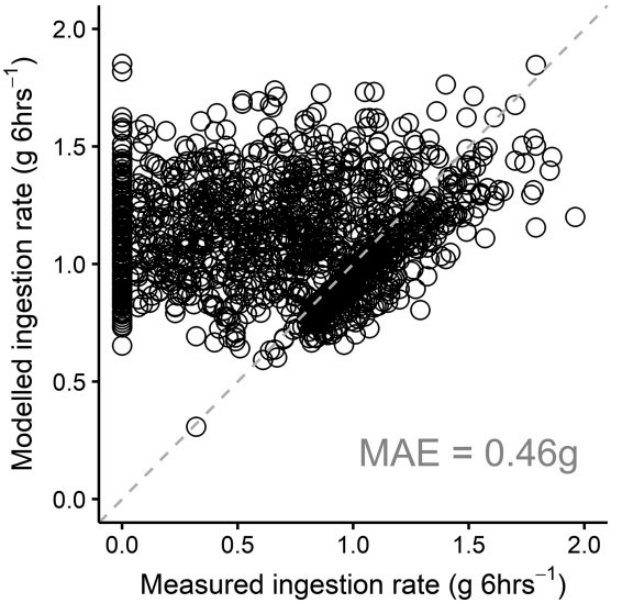

Figure 7. Measured versus modelled ingestion rate in all experimental *Liocarcinus depurator*. Dashed line is a 1:1 reference line. Modelled values were calculated using the parameters in Table 1. Mean average error (MAE) is shown.

The model showed considerably less skill in predicting *Liocarcinus* ingestion rate (Figure 7). Observed ingestion rate showed a great deal of variation over the course of the experiment, which is not captured in the model; measured ingestion over a 6-h feeding period varied between 0 and 1.96 g wet mass squid ingested, whereas model predictions ranged from 0.29 to 1.84 g wet mass squid ingested. The vertical line of points at 0 on the *x*-axis represents the animals that did not feed during at least one of the 6 h feeding periods—some of these animals would have moulted over the course of the experiment and would not have fed immediately before or after ecdysis (Figure 7). The slope of points visible just under the 1:1 reference line (Figure 7) represents those animals that ingested all the food that was presented to them.

Modelled rates of oxygen consumption demonstrated less variability than the measured rates (Figure 8). Of the eight animals measured, six were assumed to be in the intermoult stage of the moult cycle, while two had moulted within 48 h prior to having O_2 consumption measured (black filled circles, Figure 8). However, one of the animals assumed to be in the IP had a very high rate of O_2 consumption (grey filled circle, Figure 8) perhaps suggesting that it was approaching a moult. Measurements for this individual were taken on the last day of the experiment so it is unknown whether or not it moulted soon after these observations were made. An independent test of model skill when considering all eight animals measured showed a fairly large discrepancy between measured and modelled rates (MAE 0.02 µmol O_2 $gM_W^{-1}\,min^{-1}$ consumed). When excluding the animals with higher rates, however, MAE dropped to 0.01 µmol O_2 consumed $gM_W^{-1}\,min^{-1}$).

Discussion

Model performance

A simple DEB model was adequately parameterized for the decapod species *Liocarcinus depurator*. Statistical tests of the model

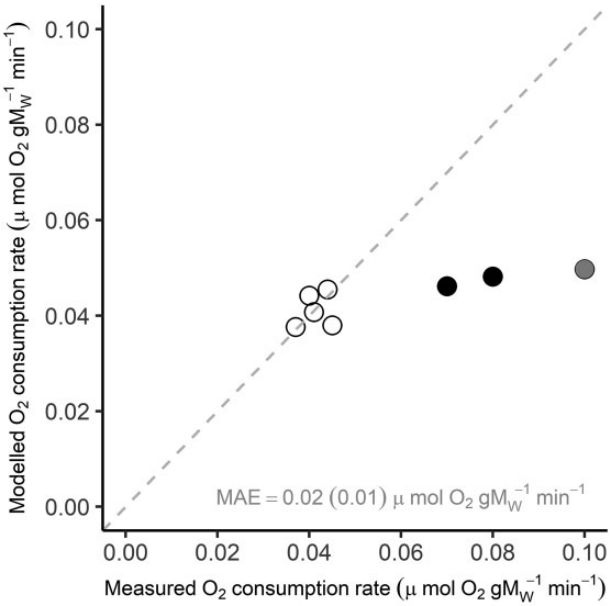

Figure 8. Measured versus modelled oxygen consumption rate for *Liocarcinus depurator*. Modelled values were calculated using the parameters in Table 1. Unfilled circles are animals that are assumed to be in the intermoult stage of the moult cycle. Black filled circles represent animals that moulted within 48 h previous to having O_2 consumption measured. Grey filled circle represents an animal that had not moulted over the course of the experiment, but was assumed to have been approaching a moult due to the very high rate of O_2 consumption measured. Mean average error (MAE) is shown. Figure in parentheses is the value of MAE when the three animals represented by filled circles are not considered. Dashed line is a 1:1 reference line.

showed that it made good predictions for the increase in wet mass during a moult, and for oxygen consumption, but lacked skill in predicting ingestion rates. By combining the DEB framework with empirical data collected specifically for modelling purposes, a set of parameters (Table 1) were estimated that describe the dynamics of physiological processes related to growth and maintenance, in particular the dynamics of the moult.

A critical factor for moult dynamics in this model was the carbon mass/wet mass ratio (α), with animals being assigned a pre-/post-moult threshold of 0.13 and 0.2, respectively (Figure 3). This ratio was also used to calculate the MI and IP of an individual crab. The independent statistic used to assess model skill in capturing moult dynamics find an acceptably low deviation (MAE = 1.24 g) between predicted and observed values for wet mass in individuals which moulted over the course of the study (Figure 6a), which suggests that α is not only a simple indicator of an individual's moult stage, but is also a powerful tool in constraining the upper limits of wet mass increase during a moult. Furthermore, when the model was run again without the "moult extension"—in effect run as a standard, if simplified, DEB model—deviations between predicted and observed values for wet mass increased (MAE = 2.93 g, Figure 6b). This would lend credence to the notion that this simple extension to DEB theory can improve predictions of growth in crustaceans by accounting for the dynamics of the moult. Once parameterized, the standard DEB model generates properties of the individual such as maximum body size. This allows the validity of the parameters to be evaluated, based on whether these "implied properties" are consistent with what is known about the life history of the species. Our model does not generate these data, so the parameters cannot be evaluated in this way, but comparison between the parameters presented here with those of the related portunid *Carcinus maenas* showed that most parameters for *C. maenas* were within 1 *SD* of the mean of those for *Liocarcinus*. This would suggest that our model parameters are valid, but a further iteration of the model in which life history properties are generated would be useful. The only other DEB model in the literature which explicitly considers moult dynamics in crustaceans is that of Ananthasubramaniam *et al.* (2015). A direct comparison between the different "moult extensions" utilized by those authors and the one presented here is beyond the scope of this article, but given that both models are built on a DEB framework, future work which tests the performance of the two approaches on the same data is possible, and would certainly be informative.

Model skill with regards to ingestion was fairly poor, with a MAE of 0.46 g (Figure 7). This is a reflection of the fact that observed ingestion rate was very variable, which was not captured in the model. This is perhaps unsurprising when considering the fact that the ingestion rate used in the model was a mean rate for all experimental animals. When there is substantial variation between individuals, the ingestion rate of the average crab can deviate considerably from the mean rate of the whole group. There is significant evidence that feeding activity in crustaceans is driven by circadian rhythms, particularly light (Reymond and Lagardère, 1990; Cannicci *et al.*, 1996; Focken *et al.*, 1998; Soares *et al.*, 2005) and tidal (Hunter and Naylor, 1993; Chatterton and Williams, 1994; Cannicci *et al.*, 1996) rhythms, which was not accounted for in the model. While these circadian rhythms may account for any temporal variations in maximum ingestion, they do not explain the differences in individual ingestion observed. However, it has been documented that feeding activity can be triggered or inhibited in individual animals depending on metabolic requirements. For example, it is well established that crustaceans in the premoult stage stop feeding (O'Halloran and O'Dor, 1988; Mantelatto and Christofoletti, 2001; Endo and Yamano, 2006).

It is evident that further work is needed to better understand the variability exhibited in feeding behaviour in *Liocarcinus*, so that this variability can be better accounted for in the model. While it is unlikely that that the model will ever capture the full variability of feeding behaviour in crustaceans, it is likely that accounting for the moult duration and the associated suppression in feeding regime may improve the modelled output to some degree.

The range of values measured for oxygen consumption in this experiment is indicative of the fact that respiration in decapods changes depending on the moult stage of an individual, with animals immediately pre- and post-moult exhibiting high O_2 consumption, and individuals mid cycle showing lower values (Alcaraz and Sarda, 1981; Penkoff and Thurberg, 1982; Stern and Cohen, 1982; Carvalho and Phan, 1998). Of the animals measured here, two had moulted within the 48 h previous to measurements being taken, which would explain the higher rates of O_2 consumption measured, and which the model failed to capture (Figure 8, black filled circles). Similarly, the individual with the highest value for O_2 consumption may have been approaching a moult (Figure 8, grey filled circle). However, oxygen consumption can vary for reasons besides moult stage, such as disease or

parasite burden (Schuwerack *et al.*, 2001), and it is possible that the very high oxygen consumption recorded in this individual was a reflection of some kind of disease related physiological stress. Equally, while those crabs with the lower oxygen consumption rates were assumed to be mid cycle [i.e. intermoult stage C based on the Drach staging system (Drach and Tchernigovtzeff, 1967)], and while there is a method for moult staging *Liocarcinus depurator* (Abello, 1989), due to practical considerations (i.e. the need for destructive sampling to accurately identify the pre-moult D_2–D_4 stage) and time constraints, none of the experimental animals were formally moult staged. Finally it should be noted that relatively few measurements were taken, and more data would be useful to better constrain the model.

The model predictions for oxygen consumption showed good agreement with observed values for those animals with the lower rates (Figure 8, unfilled circles), with a MAE of 0.01 µmol O_2 consumed $gM_W^{-1}\,min^{-1}$ when the three outliers were not considered in the analysis. When all eight animals were considered however, model skill decreased, and MAE increased to 0.02 µmol O_2 $gM_W^{-1}\,min^{-1}$ consumed. Clearly, further development is needed to ensure that the variability in oxygen consumption exhibited by crustaceans over the course of the moult cycle is accurately captured in the model.

Future model development

While this model represents a promising start to modelling crustacean moult dynamics, it requires further development. The primary limitations relate to the fact that the model currently does not capture the changes ingestion (Figure 7) and oxygen consumption rate (Figure 8) that occur as an animal progresses through the moult cycle. In order to improve model performance in these areas it is necessary to build a true "moulting period" into the model code, which causes the suppression of feeding and an increase in O_2 consumption. While O_2 consumption is an output of the model, and so cannot be coupled to the moult cycle directly, model parameters affecting O_2 consumption (e.g. maintenance rate k_M) can be. By coupling maintenance and ingestion rates to α both ingestion and O_2 consumption will change with the increase in α as an animal approaches moult.

The model in its current form does not follow the mobilized flux from the reserve to the reproductive buffer (1 − kappa) once it has been allocated—in effect, the model is representative for juvenile individuals that allocate to maturation but not reproduction. In order to explore this more fully, and to ensure that the model can have applications at the population level, the next iteration must utilize the existing DEB framework to track the energy allocated to the reproductive buffer, as well as the reproduction process itself. Again, an accurate model of moulting will be essential to get this right. Moult is critical to reproduction in many crustacean taxa, with the two being coordinated in a variety of ways (Raviv *et al.*, 2008), and influenced by environmental conditions. For example, there is evidence to suggest seasonal moulting as a precursor to a breeding season in some species. In the spiny lobster *Jasus edwardsii* (Hutton, 1875) in northeast New Zealand, both males and females had seasonal moulting periods (October/November for males, April/June for females). Females would moult immediately prior to mating, while males moulted earlier to ensure that they were in intermoult during the mating season (MacDiarmid, 1989). In temperate areas, the presence of a maximum number of brachyuran crabs of several species undergoing ecdysis in the summer has been observed by various authors (Abello, 1989; Fernández *et al.*, 1991) and the number of ovigerous females is often inversely proportional to the number of females in the moult stage (Abello, 1989; Fernández *et al.*, 1991), suggesting that these species may have a "fixed" seasonal moult in which copulation takes place. Additionally, ovigerous females do not moult, so the number of egg batches a female releases can affect moult timing. Several species (including *Liocarcinus depurator*) can spawn multiple times between moults, so the IP becomes dependent on egg incubation time, which is itself influenced by temperature (Hamasaki, 2003; Wehrtmann and López, 2003). Given the strength of this link between reproduction and moult, it is possible that, in some species, moult is not solely dependent on energetic factors (e.g. α). It may be that, during "fixed" seasonal moults, the reproductive buffer (Figure 1) plays a role in moult dynamics. This is perhaps more likely in those species exhibiting parturial moults, in which the ovaries begin to develop during the previous moult cycle and mature ovaries are carried through ecdysis, so that oviposition can occur immediately after mating. The implementation of the equations governing this reproductive buffer would allow further exploration of the role (if any) it plays in crustacean moulting.

Potential applications

The most obvious application of the model in its current form is in crustacean aquaculture. For example, it can be used to assess which production method (e.g. feeding regime) is likely to produce the fastest growth. Similarly, it can provide insights into optimal conditions (e.g. temperature) for production. It is possible that this model could be used for assessing suitable sites for sea-based container culture projects for crustaceans, such as the Lobster Grower 2 (LG2) project (www.lobstergrower.co.uk). A bio-energetic model such as the one presented here, which specifically links crustacean moulting and growth to environmental parameters, may be very useful in selecting sites that would offer the best possible conditions in which to rear juvenile lobsters. The standard DEB model is already proven to be useful in this regard, having been previously applied to evaluate the carrying capacities of marine ecosystems and evaluate their potential for bivalve aquaculture (Thomas *et al.*, 2011).

A serious problem in crustacean aquaculture is disease (Stentiford *et al.*, 2012). While this model cannot elucidate the specific responses of the crustacean immune system to pathogens, it may be of assistance in mitigating against their effects. The model can be used to quantify the effects of infection on the energy budget of the host, as has been shown for the standard DEB model in previous studies on bivalves (Flye-Sainte-Marie *et al.*, 2009). Once an effect on a DEB parameter has been quantified, can a change in feeding regime or food quality compensate to ensure continued growth? Similarly, how do commonly used immunostimulants affect parameters? Immunostimulants are proposed to enhance disease resistance in cultured species, but it is clear that their effectiveness varies with different host species, delivery methods, and types of pathogen (Rowley and Pope, 2012; Traifalgar *et al.*, 2013). Additionally, there are cogent reasons why the use of these compounds over prolonged periods may actually be detrimental to the host animal (Smith *et al.*, 2003). It may be possible to use the model to balance prophylactic efficacy of a given compound against its effect on model parameters. This model could also be useful in providing accurate

estimates of growth for use in stock assessment models for crustacean capture fisheries. While there are several growth models currently used as a basis for stock assessment in crustacean fisheries, only one explicitly considers temperature as a factor in growth, and none consider food availability. Given that both of these factors are critical drivers of growth in poikilotherms, a model that can account for changing food availability and environmental conditions would be a useful addition to the modelling toolkit of fisheries managers. Additionally, one of the more widely used of the current models—the moult process model—can produce misleading growth curves for lower latitude crustaceans as they do not generally exhibit significant seasonal moulting (Chang *et al.*, 2012).

Development of the reproductive side of the model will provide a direct link to population level processes, such as fecundity and reproductive output, as well as the effects of stressors (environmental and anthropogenic) on reproduction. This could again be useful in stock assessments of crustacean fisheries, as well as having broader applications in the fields of benthic ecology and ecological modelling. For example, it could be used to explore population and ecosystem level consequences of changes in temperature and food availability under climate change. This model could also be useful in ecotoxicology studies, where *Daphnia magna* is a standard test species. Many toxicological endpoints, including effects on reproductive output, are potentially affected by variations in moult dynamics (Ananthasubramaniam *et al.*, 2015), so a DEB model which can account for these variations has potential advantages. Finally, while we have focussed here only on crustaceans, there is no reason why the "moult extension" presented in this model cannot be more widely applied across the entire phylum of Arthropoda.

Conclusion

This article presents a framework toward developing a mechanistic model of moult dynamics and growth in crustaceans, a group in which growth modelling has historically been problematic. While the current model needs further development, we believe this approach shows promise, and could be used to explore a process that is fundamental to the life history of crustaceans. Furthermore, it could prove to be a valuable tool for use in the management of crustacean capture fisheries and aquaculture, where accurate estimates of growth are critical to providing optimal management advice for developing sustainable fisheries.

Supplementary data

Supplementary material is available at the *ICESJMS* online version of the manuscript.

Acknowledgements

This work was supported by the National Environment Research Council via the SPITFIRE studentship [grant number NE/L002531/1]. We are grateful to the crew of the RV Plymouth Quest for animal collection, and to Joana Nunes for providing practical assistance with experimental setup.

References

Abello, P. 1989. Reproduction and moulting in Liocarcinus depurator (Linnaeus, 1758) (Brachyura: Portunidae) in the northwestern Mediterranean Sea. Scientia Marina, 53: 127–134.

Ackefors, H., Castell, J. D., Boston, L. D., Räty, P., and Svensson, M. 1992. Standard experimental diets for crustacean nutrition research. II. Growth and survival of juvenile crayfish *Astacus astacus* (Linné) fed diets containing various amounts of protein, carbohydrate and lipid. Aquaculture, 104: 341–356.

Alcaraz, M., and Sarda, F. 1981. Oxygen consumption by Nephrops norvegicus (L.), (Crustacea: Decapoda) in reationship with its moult stage. Journal of Experimental Marine Biology and Ecology, 54: 113–118.

AmP. n.d.. Add my Pet, online database of DEB parameters; implied properties and referenced underlying data. https://www.bio.vu.nl/thb/deb/deblab/add_my_pet/ (last accessed 3 July 2018).

Ananthasubramaniam, B., McCauley, E., Gust, K. A., Kennedy, A. J., Muller, E. B., Perkins, E. J., and Nisbet, R. M. 2015. Relating suborganismal processes to ecotoxicological and population level endpoints using a bioenergetic model. Ecological Applications, 25: 1691–1710.

Bai, N., Zhang, W., Mai, K., Wang, X., Xu, W., and Ma, H. 2010. Effects of discontinuous administration of β-glucan and glycyrrhizin on the growth and immunity of white shrimp Litopenaeus vannamei. Aquaculture, 306: 218–224.

Boudreau, S. A., and Worm, B. 2012. Ecological role of large benthic decapods in marine ecosystems: a review. Marine Ecology Progress Series, 469: 195–213.

Bozinovic, F., and Pörtner, H. 2015. Physiological ecology meets climate change. Ecology and Evolution, 5: 1025–1030.

Bruggeman, J. 2017. DEB species explorer. http://server1.pml.ac.uk/traitexplorer/deb.shtml (last accessed 14 January 2018).

Brylawski, B. J., and Miller, T. J. 2006. Temperature-dependent growth of the blue crab (*Callinectes sapidus*): a molt process approach. Canadian Journal of Fisheries and Aquatic Sciences, 63: 1298–1308.

Buchholz, C. M., Buchholz, F., and Tarling, G. A. 2006. On the timing of moulting processes in reproductively active Northern krill *Meganyctiphanes norvegica*. Marine Biology, 149: 1443–1452.

Caddy, J. F. 2003. Scaling elapsed time: an alternative approach to modelling crustacean moulting schedules? Fisheries Research, 63: 73–84.

Campos, J., Van der Veer, H. W., Freitas, V., and Kooijman, S. A. L. M. 2009. Contribution of different generations of the brown shrimp *Crangon crangon* (L.) in the Dutch Wadden Sea to commercial fisheries: a dynamic energy budget approach. Journal of Sea Research, 62: 106–113.

Cannicci, S., Dahdouh-Guebas, F., Dyane, A., and Vannini, M. 1996. Natural diet and feeding habits of *Thalamita crenata* (Decapoda: Portunidae). Journal of Crustacean Biology, 16: 678–683.

Carvalho, P. S. M., and Phan, V. N. 1998. Oxygen consumption and ammonia excretion during the moulting cycle in the shrimp *Xiphopenaeus kroyeri*. Comparative Biochemistry and Physiology - A Molecular and Integrative Physiology, 119: 839–844.

Castro, M. 1992. A methodology for obtaining information on the age structure and growth rates of the Norway lobster, *Nephrops norvegicus* (L.) (Decapoda, Nephropoidea). Crustaceana, 63: 29–43.

Cawthorn, D.-M., and Hoffman, L. C. 2017. Deceit with decapods? Evaluating labelling accuracy of crustacean products in South Africa. Food Control, 73: 741–753.

Chang, Y. J., Sun, C. L., Chen, Y., and Yeh, S. Z. 2012. Modelling the growth of crustacean species. Reviews in Fish Biology and Fisheries, 22: 157–187.

Chatterton, T. D., and Williams, B. G. 1994. Activity patterns of the New Zealand cancrid crab Cancer novaezelandiae (Jacquinot) in the field and laboratory. Journal of Experimental Marine Biology and Ecology, 178: 261–274.

Chen, Y., and Kennelly, S. J. 1999. Growth of spanner crabs, *Ranina ranina*, off the east coast of Australia. Marine and Freshwater Research, 50: 319–325.

Cuzin-Roudy, J., and Buchholz, F. 1999. Ovarian development and spawning in relation to the moult cycle in Northern krill,

Meganyctiphanes norvegica (Crustacea: Euphausiacea), along a climatic gradient. Marine Biology, 133: 267–281.

Drach, P., and Tchernigovtzeff, C. 1967. Sur la methode de détermination des stades d'intermue et son application générale aux crustacés. Vie Milieu, 18: 595–607.

Easton, M. D. L., and Misra, R. K. 1988. Mathematical representation of crustacean growth. ICES Journal of Marine Science, 45: 61–72.

Ehrhardt, N. M. 2008. Estimating growth of the Florida spiny lobster, *Panulirus argus*, from molt frequency and size increment data derived from tag and recapture experiments. Fisheries Research, 93: 332–337.

Elner, R. W., and Beninger, P. G. 1995. Multiple reproductive strategies in snow crab, Chionoecetes opilio: physiological pathways and behavioral plasticity. Journal of Experimental Marine Biology and Ecology, 193: 93–112.

Endo, Y., and Yamano, F. 2006. Diel vertical migration of *Euphausia pacifica* (Crustacea, Euphausiacea) in relation to molt and reproductive processes, and feeding activity. Journal of Oceanography, 62: 693–703.

Ettershank, G. 1983. Age structure and cyclical annual size change in the Antarctic krill, *Euphausia superba* Dana. Polar Biology, 2: 189–193.

FAO. 2016. State of world fisheries and aquaculture 2016. Food & Agriculture Org.

Fernández, L., González-Gurriarán, E., and Freire, J. 1991. Population biology of *Liocarcinus depurator* (Brachyura, Portunidae) in mussel raft culture areas in the Ria De Arousa (Galicia, Nw Spain). Journal of the Marine Biological Association of the United Kingdom, 71: 375–390.

Flye-Sainte-Marie, J., Jean, F., Paillard, C., and Kooijman, S. A. L. M. 2009. A quantitative estimation of the energetic cost of brown ring disease in the Manila clam using Dynamic Energy Budget theory. Journal of Sea Research, 62: 114–123.

Focken, U., Groth, A., Coloso, R. M., and Becker, K. 1998. Contribution of natural food and supplemental feed to the gut content of *Penaeus monodon* Fabricius in a semi-intensive pond system in the Philippines. Aquaculture, 164: 105–116.

Hamasaki, K. 2003. Effects of temperature on the egg incubation period, survival and developmental period of larvae of the mud crab *Scylla serrata* (Forskål)(Brachyura: Portunidae) reared in the laboratory. Aquaculture, 219: 561–572.

Harley, C. D. G., and Paine, R. T. 2009. Contingencies and compounded rare perturbations dictate sudden distributional shifts during periods of gradual climate change. Proceedings of the National Academy of Sciences of the United States of America, 106: 11172–11176.

Harley, C. D. G., Randall Hughes, A., Hultgren, K. M., Miner, B. G., Sorte, C. J. B., Thornber, C. S., Rodriguez, L. F., *et al.* 2006. The impacts of climate change in coastal marine systems. Ecology Letters, 9: 228–241.

Helmuth, B., Broitman, B. R., Blanchette, C. A., Gilman, S., Halpin, P., Harley, C. D. G., and O'Donnell, M. J. 2006. Mosaic patterns of thermal stress in the rocky intertidal zone: implications for climate change. Ecological Monographs, 76: 461–479.

Hiddink, J. G., and Ter Hofstede, R. 2008. Climate induced increases in species richness of marine fishes. Global Change Biology, 14: 453–460.

Hoegh-Guldberg, O. 1999. Climate change, coral bleaching and the future of the world's coral reefs. Marine and Freshwater Research, 50: 839–866.

Hoggarth, D. D. 2006. Stock assessment for fishery management: a framework guide to the stock assessment tools of the fisheries management and science programme. Food & Agriculture Org.

Hunter, E., and Naylor, E. 1993. Intertidal migration by the shore crab *Carcinus maenas*. Marine Ecology Progress Series, 101: 131.

Iguchi, N., and Ikeda, T. 1995. Growth, metabolism and growth efficiency of a euphasiis crustacean *Euphausia pacifica* in the southern Japan Sea, as influenced by temperature. Journal of Plankton Research, 17: 1757–1769.

Iguchi, N., and Ikeda, T. 2004. Effects of temperature on metabolism, growth and growth efficiency of *Thysanoessa longipes* (Crustacea: Euphausiacea) in the Japan Sea. Journal of Plankton Research, 27: 1–10.

Jager, T., and Ravagnan, E. 2015. Parameterising a generic model for the dynamic energy budget of Antarctic krill *Euphausia superba*. Marine Ecology Progress Series, 519: 115–128.

Jager, T., and Ravagnan, E. 2016. Modelling growth of northern krill (*Meganyctiphanes norvegica*) using an energy-budget approach. Ecological Modelling, 325: 28–34.

Jager, T., and Zimmer, E. I. 2012. Simplified Dynamic Energy Budget model for analysing ecotoxicity data. Ecological Modelling, 225: 74–81.

Jager, T., Salaberria, I., and Hansen, B. H. 2015. Capturing the life history of the marine copepod *Calanus sinicus* into a generic bioenergetics framework. Ecological Modelling, 299: 114–120.

Kilada, R., and Driscoll, J. G. 2017. Age determination in crustaceans: a review. Hydrobiologia, 799: 21–36.

Kim, S., Pang, Z., Seo, H., Cho, Y., Samocha, T., and Jang, I. 2014. Effect of bioflocs on growth and immune activity of Pacific white shrimp, L itopenaeus vannamei postlarvae. Aquaculture Research, 45: 362–371.

Klein Breteler, W. C. M. 1975. Food consumption, growth and energy metabolism of juvenile shore crabs, *Carcinus maenas*. Netherlands Journal of Sea Research, 9: 255–272.

Kooijman, S. , and a L. M. 2010. Dynamic energy budget theory for metabolic organisation: summary of concepts of the third edition. Water, 365: 68.

Leland, A. V. 2002. A new apex predator in the Gulf of Maine? Large, mobile crabs (Cancer borealis) control benthic community structure. Electronic Theses and Dissertations, 143. https://digitalcommons.library.umaine.edu/cgi/viewcontent.cgi?article=1150&context=etd

Lemos, D., Phan, V. N., and Alvarez, G. 2001. Growth, oxygen consumption, ammonia-N excretion, biochemical composition and energy content of *Farfantepenaeus paulensis* Peŕez-Farfante (Crustacea, Decapoda, Penaeidae) early postlarvae in different salinities. Journal of Experimental Marine Biology and Ecology, 261: 55–74.

MacDiarmid, A. B. 1989. Moulting and reproduction of the spiny lobster *Jasus edwardsii* (Decapoda: Palinuridae) in northern New Zealand. Marine Biology, 103: 303–310.

Mantelatto, F. L. M., and Christofoletti, R. A. 2001. Natural feeding activity of the crab *Callinectes ormatus* (Portunidae) in Ubatuba Bay (Sao Paulo, Brazil): influence of season, sex, sizaa and molte stage. Marine Biology, 138: 585–594.

Martin, B. T., Jager, T., Nisbet, R. M., Preuss, T. G., and Grimm, V. 2013. Predicting population dynamics from the properties of individuals: a cross-level test of dynamic energy budget theory. The American Naturalist, 181: 506–519.

Mauchline, J. 1977. Growth of shrimps, crabs and lobsters – an assessment. ICES Journal of Marine Science, 37: 162–169.

McGaw, I. J., and Whiteley, N. M. 2012. Effects of acclimation and acute temperature change on specific dynamic action and gastric processing in the green shore crab, *Carcinus maenas*. Journal of Thermal Biology, 37: 570–578.

Nicol, S. 2000. Understanding krill growth and aging: the contribution of experimental studies. Canadian Journal of Fisheries and Aquatic Sciences, 57: 168–177.

Nicol, S., Stolp, M., Cochran, T., Geijsel, P., and Marshall, J. 1992. Growth and shrinkage of Antarctic krill *Euphausia superba* from the Indian Ocean sector of the Southern Ocean during summer. Marine Ecology Progress Series, 89: 175–181.

Nisbet, R. M., McCauley, E., Gurney, W. S. C., Murdoch, W. W., and Wood, S. N. 2004. Formulating and testing a partially specified dynamic energy budget model. Ecology, 85: 3132–3139.

O'Halloran, M. J., and O'Dor, R. K. 1988. Molt cycle of male snow crabs, *Chionoecetes opilio*, from observations of external features, setal changes, and feeding behavior. Journal of Crustacean Biology, 8: 164–176.

Paul, A. J., and Fuji, A. 1989. Bioenergetics of the Alaskan crab *Chionoecetes bairdi* (Decapoda: Majidae). Journal of Crustacean Biology, 9: 25–36.

Pearson, G. A., Lago-Leston, A., and Mota, C. 2009. Frayed at the edges: selective pressure and adaptive response to abiotic stressors are mismatched in low diversity edge populations. Journal of Ecology, 97: 450–462.

Penkoff, S. J., and Thurberg, F. P. 1982. Changes in oxygen consumption of the American lobster, *Homarus americanus*, during the molt cycle. Comparative Biochemistry and Physiology Part A: Physiology, 72: 621–622.

Place, S. P., O'Donnell, M. J., and Hofmann, G. E. 2008. Gene expression in the intertidal mussel *Mytilus californianus*: physiological response to environmental factors on a biogeographic scale. Marine Ecology Progress Series, 356: 1–14.

Poloczanska, E. S., Brown, C. J., Sydeman, W. J., Kiessling, W., Schoeman, D. S., Moore, P. J., Brander, K., *et al.* 2013. Global imprint of climate change on marine life. Nature Climate Change, 3: 919.

Pörtner, H. O., and Knust, R. 2007. Climate change affects marine fishes through the oxygen limitation of thermal tolerance. Science, 315: 95–97.

Quetin, L. B., and Ross, R. M. 1991. Behavioral and physiological characteristics of the Antarctic krill, *Euphausia superba*. American Zoologist, 31: 49–63.

Quijón, P., and Snelgrove, P. 2005. Differential regulatory roles of crustacean predators in a sub-Arctic, soft-sediment system. Oecologia, 144: 137–149.

Raviv, S., Parnes, S., and Sagi, A. 2008. Coordination of reproduction and molt in decapods. *In* Reproductive Biology of Crustaceans, 365–390. Ed. by Mente, E. CRC Press, Boca Raton.

Reymond, H., and Lagardère, J. P. 1990. Feeding rhythms and food of *Penaeus japonicus* bate (crustacea, penaeidae) in salt marsh ponds; role of halophilic entomofauna. Aquaculture, 84: 125–143.

Rowley, A. F., and Pope, E. C. 2012. Vaccines and crustacean aquaculture—A mechanistic exploration. Aquaculture, 334–337: 1–11.

Sainte-Marie, B., Gosselin, T., Sévigny, J.-M., and Urbani, N. 2008. The snow crab mating system: opportunity for natural and unnatural selection in a changing environment. Bulletin of Marine Science, 83: 131–161.

Sang, H. M., Fotedar, R., and Filer, K. 2011. Effects of dietary mannan oligosaccharide on the survival, growth, immunity and digestive enzyme activity of freshwater crayfish, *Cherax destructor* Clark (1936). Aquaculture Nutrition, 17: e629–e635.

Schuwerack, P.-M., Lewis, J. W., and Jones, P. W. 2001. Pathological and physiological changes in the South African freshwater crab *Potamonautes warreni* Calman induced by microbial gill infestations. Journal of Invertebrate Pathology, 77: 269–279.

Seear, P. J., Tarling, G. A., Burns, G., Goodall-Copestake, W. P., Gaten, E., Özkaya, Ö., and Rosato, E. 2010. Differential gene expression during the moult cycle of Antarctic krill (*Euphausia superba*). BMC Genomics, 11: 582.

Silliman, B. R., and Bertness, M. D. 2002. A trophic cascade regulates salt marsh primary production. Proceedings of the National Academy of Sciences of the United States of America, 99: 10500–10505.

Smith, M. T., and Addison, J. T. 2003. Methods for stock assessment of crustacean fisheries. Fisheries Research, 65: 231–256.

Smith, V. J., Brown, J. H., and Hauton, C. 2003. Immunostimulation in crustaceans: does it really protect against infection? Fish & Shellfish Immunology, 15: 71–90.

Smyth, T., Fishwick, J., Bell, T., and Widdicombe, S. 2015. The western channel observatory - collecting rare and precious time series from photons to fish. The Magazine of the Challenger Society for Marine Science, 21: 32–34.

Soares, R., Peixoto, S., Wasielesky, W., and D'Incao, F. 2005. Feeding rhythms and diet of *Farfantepenaeus paulensis* under pen culture in Patos Lagoon estuary, Brazil. Journal of Experimental Marine Biology and Ecology, 322: 167–176.

Somerton, D. A. 1980. Fitting straight lines to Hiatt growth diagrams: a re-evaluation. ICES Journal of Marine Science, 39: 15–19.

Steneck, R. S., Vavrinec, J., and Leland, A. V. 2004. Accelerating trophic-level dysfunction in kelp forest ecosystems of the western North Atlantic. Ecosystems, 7: 323–332.

Stentiford, G. D., Neil, D. M., Peeler, E. J., Shields, J. D., Small, H. J., Flegel, T. W., Vlak, J. M., *et al.* 2012. Disease will limit future food supply from the global crustacean fishery and aquaculture sectors. Journal of Invertebrate Pathology, 110: 141–157.

Stern, S., and Cohen, D. 1982. Oxygen consumption and ammonia excretion during the molt cycle of the freshwater prawn *Macrobrachium rosenbergii* (De Man). Comparative Biochemistry and Physiology Part A: Physiology, 73: 417–419.

Taylor, D. L., and Peck, M. A. 2004. Daily energy requirements and trophic positioning of the sand shrimp Crangon septemspinosa. Marine Biology, 145: 167–177.

Thomas, Y., Mazurié, J., Alunno-Bruscia, M., Bacher, C., Bouget, J.-F., Gohin, F., Pouvreau, S., *et al.* 2011. Modelling spatio-temporal variability of *Mytilus edulis* (L.) growth by forcing a dynamic energy budget model with satellite-derived environmental data. Journal of Sea Research, 66: 308–317.

Traifalgar, R. F. M., Corre, V. L., and Serrano, A. E. 2013. Efficacy of dietary immunostimulants to enhance the immunological responses and Vibriosis resistance of juvenile *Penaeus monodon*. Journal of Fisheries and Aquatic Science, 8: 340–352.

van der Meer, J. 2006. An introduction to Dynamic Energy Budget (DEB) models with special emphasis on parameter estimation. Journal of Sea Research, 56: 85–102.

Wainwright, T. C., and Armstrong, D. A. 1993. Growth patterns in the Dungeness crab (*Cancer magister* Dana): synthesis of data and comparison of models. Journal of Crustacean Biology, 13: 36–50.

Wehrtmann, I. S., and López, G. A. 2003. Effects of temperature on the embryonic development and hatchling size of *Betaeus emarginatus* (Decapoda: Caridea: Alpheidae). Journal of Natural History, 37: 2165–2178.

West, A., McGrorty, S., Caldow, R., Durell, S., Yates, M., and Stillman, R. 2004. Sampling macro-invertebrates on intertidal flats to determine the potential food supply for waders. NERC/Centre for Ecology & Hydrology.

Wyban, J., Walsh, W. A., and Godin, D. M. 1995. Temperature effects on growth, feeding rate and feed conversion of the Pacific white shrimp (*Penaeus vannamei*). Aquaculture, 138: 267–279.

Zacherl, D., Gaines, S. D., and Lonhart, S. I. 2003. The limits to biogeographical distributions: insights from the northward range extension of the marine snail, *Kelletia kelletii* (Forbes, 1852). Journal of Biogeography, 30: 913–924.

Handling editor: Erika J Eliasson